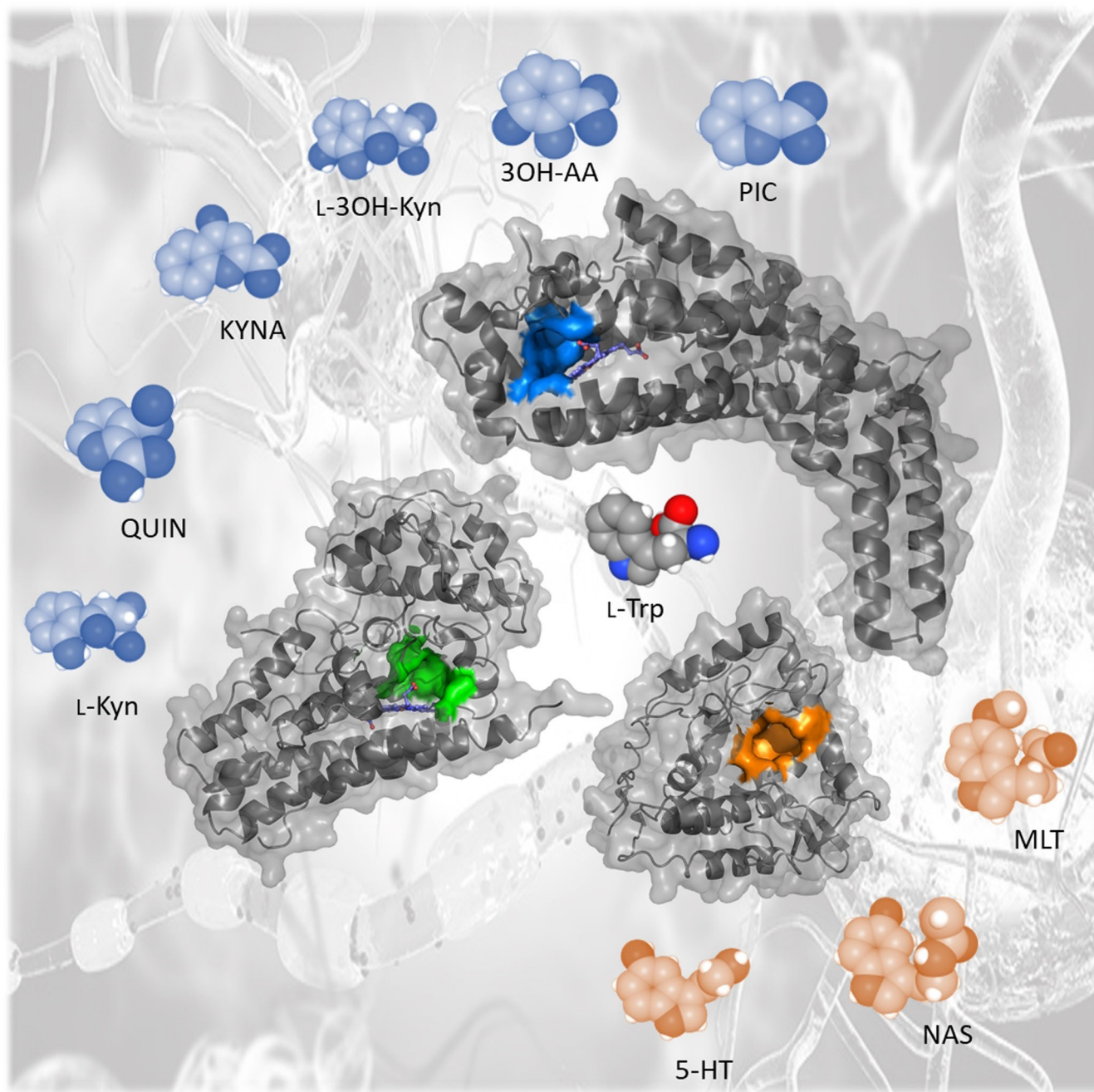


One Key and Multiple Locks: Substrate Binding in Structures of Tryptophan Dioxygenases and Hydroxylases

Andrea Mammoli,^[a] Alessandra Riccio,^[a] Elisa Bianconi,^[a] Alice Coletti,^[b] Emidio Camaioni,^[a] and Antonio Macchiarulo*^[a]



Since its discovery at the beginning of the past century, the essential nutrient L-Tryptophan (L-Trp) and its catabolic pathways have acquired an increasing interest in an ever wider scientific community for their pivotal roles in underlying many important physiological functions and associated pathological conditions. As a consequence, enzymes catalyzing rate limiting steps along L-Trp catabolic pathways - including IDO1, TDO, TPH1 and TPH2 - have turned to be interesting drug targets for the design and development of novel therapeutic agents for

different disorders such as carcinoid syndrome, cancer and autoimmune diseases. This article provides a fresh comparative overview on the most recent advancements that crystallographic studies, biophysical and computational works have brought on structural aspects and molecular recognition patterns of these enzymes toward L-Trp. Finally, a conformational analysis of L-Trp is also discussed as part of the molecular recognition process governing the binding of a substrate to its cognate enzymes.

1. Introduction

L-Tryptophan (L-Trp, **1**; Figure 1) is an aromatic amino acid discovered in 1901 by Hopkins and Cole from the hydrolysis of casein.^[1] It constitutes a key substrate both for protein synthesis and generation of several bioactive metabolites with important physiological functions.^[2] Since mammals lack the anabolic pathway for L-Trp, they must take this essential amino acid from diet, with a recommended daily dose of 3.5–6 mg/kg body weight.^[3,4] Out of this amount, a minor part of dietary L-Trp is used for protein synthesis, with protein degradation turnover satisfying the requirement for this purpose.^[5] The majority of dietary L-Trp is used for the production of a wide array of bioactive metabolites along specific metabolic routes which include the kynurenine (L-Kyn, **3**) pathway (KP) and the serotonin (5-HT or 5-hydroxytryptamine, **13**) pathway (SP, Figure 1).

Serotonin is a neuroactive metabolite which regulates important functions in central nervous system (CNS) and peripheral districts, such as appetite, mood-anxiety, cognition, nociception, gastrointestinal activity, immune responses, and hemodynamics.^[6,7] Its biosynthesis originates from the 5-hydroxylation of L-Trp by tryptophan hydroxylase (TPH, EC.1.14.16.4) and the subsequent decarboxylation of the α -aminoacidic group by the substrate-promiscuous aromatic amino acid decarboxylase (AADC, EC.4.1.1.28), with the first reaction constituting the rate-limiting step of SP. Two isoforms of TPH have been characterized differing in kinetic properties and tissue expression.^[8] Specifically, TPH1 is expressed in enterochromaffin cells of the gut epithelium wherein serotonin is produced and released, exerting local actions and being taken

up by platelets that distribute this metabolite to peripheral districts. Moreover, TPH1 is also expressed in the pineal gland, wherein serotonin is used as precursor for the synthesis of the circadian regulators N-acetyl-serotonin (NAS, **15**) and melatonin (MLT, **16**).^[9,10]

TPH2 is expressed in the Raphe nuclei and enteric neurons, accounting for the production of serotonin as neurotransmitter of serotonergic synapses in the brain and gut, respectively.^[11,12]

Since serotonin cannot pass the blood-brain barrier, there is not a cross-talk regulation between peripheral tissues and CNS for the relative serotonergic functions. Whereas the development of small molecules potentiating the central SP could be of interest for providing novel therapeutic opportunities against psychiatric disorders, the design of peripheral TPH inhibitors is actively pursued for the therapeutic treatment of diverse disorders including hemostatic disease, inflammation, fibrosis, gastrointestinal disorders, and metabolic diseases.^[13] In this framework, the last decade has witnessed the approval by FDA

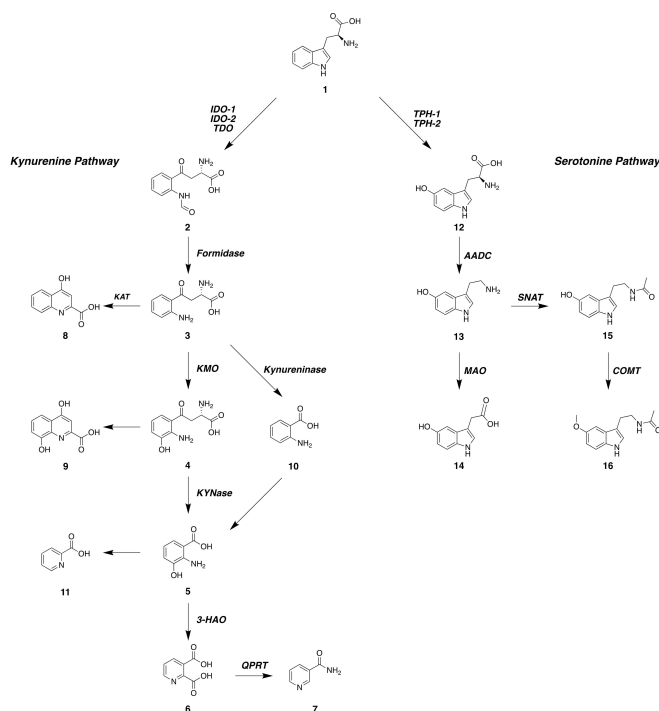


Figure 1. The kynurenine pathway and the serotonin pathway along the catabolic route of L-Trp.

[a] Dr. A. Mammoli, Dr. A. Riccio, Dr. E. Bianconi, Prof. E. Camaioni, Prof. A. Macchiariulo
 Department of Pharmaceutical Sciences,
 University of Perugia
 Via del Liceo N. 1, 06123 Perugia (Italy)
 E-mail: antonio.macchiariulo@unipg.it

[b] Dr. A. Coletti
 Department of Medicine and Surgery,
 University of Perugia
 P. le Gambuli, 06132 Perugia (Italy)

Supporting information for this article is available on the WWW under <https://doi.org/10.1002/cmdc.202100312>

© 2021 The Authors. ChemMedChem published by Wiley-VCH GmbH. This is an open access article under the terms of the Creative Commons Attribution Non-Commercial NoDerivs License, which permits use and distribution in any medium, provided the original work is properly cited, the use is non-commercial and no modifications or adaptations are made.

of the first peripheral non-selective TPH inhibitor (Telotristat ethyl) for the treatment of carcinoid syndrome.^[14,15]

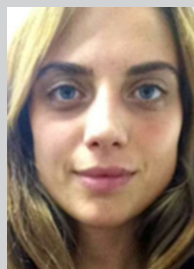
Despite the important roles of serotonin and its downstream metabolites NAS (15) and MLT (16) in CNS and peripheral tissues, studies in mammals have shown that only a

minor fraction of L-Trp available from diet enters the SP. Indeed, the largest fraction (~95%) of this essential amino acid is conveyed into the KP.^[16]

Herein, a large array of bioactive metabolites is produced starting from the conversion of L-Trp in N-formyl-kynurenine



Andrea Mammoli is a PhD fellow in Pharmaceutical Sciences at the University of Perugia. In 2017, he received his master's degree in Chemistry and Technology of Drugs at the University of Camerino. In 2018, he started his PhD joining the research group of Prof. Antonio Macchiarulo and Prof. Emidio Camaioni, working on the design, synthesis, and physicochemical characterisation of IDO1 modulators. Andrea Mammoli has been visiting scientist at the Discovery DMPK department in Aptuit, an Evotec Company, under the supervision of Dr. Stefano Fontana.



After receiving a master's degree in Pharmaceutical Biotechnology at the University of Perugia, in 2019 Alessandra Riccio joined the research group of Prof. Antonio Macchiarulo as PhD fellow. In 2019 she was awarded with the "Merk and Elsevier" prize from the Division of Medicinal Chemistry of the Young Italian Chemical Society. Her research activity is focused on the use of computer aided drug design approaches for the identification and design of small molecule modulators of conventional and non-conventional targets in immuno-oncology.



Elisa Bianconi graduated in Pharmaceutical Biotechnology in 2020 and is actually a PhD fellow in Pharmaceutical Sciences at the University of Perugia. Her research activity covers the development and use of different biophysical techniques for the study of ligand binding interactions to relevant protein targets in cancer, infectious diseases and metabolic disorders.



Alice Coletti is Post-Doctoral Researcher at Medicinal and Surgery Department of University of Perugia. In 2013, she graduated in Chemistry and Technology of Drugs at the University of Perugia. Then, in 2017, she was awarded with a PhD in Chemistry and Pharmaceutical Sciences. During her Post-Doctoral carrier, she has been actively involved in several national and international projects (ERC-2013-AdG 338954-DIDO; Italian Research Project PRIN2015, prot.20155 C2PP7; PO.FSE Umbria 2014–2020 CUP I91G18000250009; Italian Research Project PRIN2017, prot.2017B-ZEREZ 001), where she has developed and applied biophysical methods to investigate ligand binding for therapeutic targets in CNS disorders, cancer, autoimmunity, and metabolic diseases. Alice Coletti has been visiting scientist at Uppsala University (Sweden) in the research group of Prof. U. Helena Danielson, and at Biodesy Inc. (San Francisco, CA, USA).



Emidio Camaioni graduated in Chemistry and Drug Technology at the University of Camerino (Italy) under the supervision of Prof. Gloria Cristalli. After receiving the PhD in Medicinal Chemistry, in 1997, he joined the laboratory of Dr. Kenneth Jacobson at MRS/NIDDK of the National Institute of Health, Bethesda (USA) as a postdoctoral fellow. In 1999, he joined the group of Prof. Roberto Pellicciari at University of Perugia. Since 2005, he is Associate Professor at Department of Pharmaceutical Sciences (University of Perugia). His interests span in medicinal, analytical and computational chemistry fields, focusing the research activity on the design and synthesis of heterocyclic derivatives.



Antonio Macchiarulo is Full Professor of Medicinal Chemistry at the Department of Pharmaceutical Sciences of the University of Perugia (Italy). He received his PhD in Chemistry and Technology of Drugs in 2004, and was awarded with a Marie Curie fellowship (European Commission Program 'Quality of Life,' contract number: QLRI-1999-50595) at the European Bioinformatics Institute in Cambridge (UK), where he worked on the specificity of substrate recognition by enzymes. He has been member of the Scientific Committee of the European School of Medicinal Chemistry (ESMEC) and is Coordinator of the PhD program in Pharmaceutical Sciences at the University of Perugia. Antonio Macchiarulo has participated as scientific leader of research unit in several national and European research projects (ERC-2013-AdG 338954-DIDO; ERC-2017-PoC-780807-DIDO-MS; ERC-2019-PoC-899838-ENHANCIDO). His research activities cover the integration and application of computational and biophysical approaches for the design of chemical tools targeting immune checkpoint targets.

(NFK, **2**) and then L-Kyn (**3**).^[17] Specifically, this latter metabolite is the first bioactive product of the pathway that, upon binding to the Aryl hydrocarbon Receptor (AhR), regulates the expression of anti-inflammatory genes.^[18–21]

Downstream the KP, and along two specific branches that take over depending on the relative enzymes expressed in distinct cell types, L-Kyn is transformed into the neurotoxic metabolite quinolinic acid (QUIN, **6**) or into the neuroprotective metabolite kynurenic acid (KYNA, **8**).^[22] Other bioactive products of this pathway include 3-hydroxykynurenine (3OH-Kyn, **4**) and 3-hydroxyanthranilic acid (3OH-AA, **5**) that induce neuronal damage by generating reactive oxygen species,^[23,24] and picolinic acid (PIC, **11**) which is a macrophage activating ligand promoting inflammatory reactions.^[25,26] Accordingly, unbalanced production of KP metabolites has been involved in the pathogenesis of several human disorders including autoimmune diseases, inflammation, cancer, neurologic and psychiatric illnesses.^[27–31]

Of note, KP leads to the synthesis of NAD⁺ specifically in the liver, with this district accounting for more than 90% of L-Trp degradation in physiological conditions. Hence, the aforementioned bioactive metabolites are produced in extrahepatic tissues including CNS, placenta, lung and immune cells.^[16] The rate limiting step of KP consists in the oxidative opening of the indole ring of L-Trp to produce N-formyl-kynurenine (NFK, **2**).^[32] The reaction is catalyzed by tryptophan-2,3-dioxygenase (TDO, EC.1.13.11.11) and indoleamine 2,3-dioxygenases (IDO1 and IDO2, EC.1.13.11.52).^[33] Although the design and synthesis of TDO and IDO1 inhibitors is sought for the development of novel anticancer agents able to stop the tumor immuno-editing process and some of them are being evaluated in clinical settings, none of such compounds has been approved for therapy yet.^[34–36]

TDO is a homo-tetrameric enzyme which is mainly expressed in the liver and shows a high specificity toward its substrate L-Trp. Its gene expression is induced by L-Trp, tyrosine, histidine, glucocorticoids and L-Kyn.^[37] IDO1 and IDO2 are monomeric enzymes that catalyze the oxidative cleavage of a broad range of indole-bearing substrates.^[38–40] While IDO1 is ubiquitously expressed in many tissues and its expression is regulated by immunological signals,^[41,42] IDO2 is mostly expressed in murine kidney, liver, and reproductive system.^[43]

It is worth noting that NAS (**15**), the circadian bioactive metabolite produced by the serotonin pathway, has recently been shown to act as positive allosteric modulator of IDO1, providing the first evidence about a small-molecule mediated cross-talk between the two pathways of the endogenous L-Trp catabolism.^[44]

In this framework, another level of balance between SP and KP may rely on the substrate avidity of the rate limiting enzymes in those districts wherein these proteins are co-expressed. Indeed, TPH1, TPH2, TDO, IDO1 and IDO2 show different substrate's affinity to L-Trp, as evidenced by the relative Michaelis-Menden constants (K_M , Table 1), with some of them (TDO and IDO1) possessing also multiple binding sites for the substrate.^[45–47]

Table 1. Michaelis-Menten constants and catalytic rate constants of L-Trp to tryptophan hydroxylases and dioxygenases.

Enzyme	K_M [mM]	k_{cat} [s^{-1}]	Reference
hTPH1	0.023 (pH 7.0)	-	[8]
hTPH2	0.040 (pH 7.0)	-	[8]
hTDO	0.190 (pH 7.0)	2.1	[87, 111]
	0.222 (pH 8.0)	1.4	[48]
	0.120 (pH 7.0)	2.24	[49]
	0.135 (pH 8.0)	1.071	[50]
	0.021 (pH 6.5)	1.7	[88, 112]
hIDO1	0.007 (pH 8.0)	1.4	[48]
	0.023 (pH 7.4)	4.3	[57]
	0.021 (pH 6.5)	2.97	[89, 113]
hIDO2	0.022 (pH 7.5)	652 (min^{-1})	[69]
	6.809 (pH 7.5)	0.103	[89, 113]

Crystallographic, spectroscopic, biophysical and computational approaches have been instrumental to get insights into the molecular basis of the different affinity of L-Trp to some of the rate limiting enzymes of the kynurenine and serotonin pathways, unveiling specific molecular recognition and stereoselectivity patterns of the substrate to human IDO1 and TDO.^[45,47–50]

In this article we provide a survey of such studies, integrating the account with an analysis on the molecular recognition of L-Trp to human TPH1 and TPH2, as well as some new studies on the conformational properties of L-Trp that may in part affect the substrate binding affinity.

2. Structure and Substrate Binding Pockets of Tryptophan Dioxygenases

2.1. IDO1

Since the determination of the first crystal structure of IDO1 (PDB codes: 2D0T, 2D0U),^[51] an increasing number of crystallographic studies proved successful to disclose different ligand-bound and unbound forms of the enzyme that show a conserved architecture with specific ligand-induced conformational changes of secondary motifs.^[52] According to these studies, the heme-containing catalytic site is located into a large domain of IDO1, whereas two functional immunoreceptor tyrosine-based inhibition motifs (ITIM, Tyr111, Tyr249) are placed in a small domain which, upon phosphorylation by Src kinases, accounts for the non-catalytic signaling functions of the enzyme (Figure 2A).^[53] A further conserved phosphorylation site is located at YENM motif (residues 145–148) which protrudes from the small domain toward α -helix B of the large domain (Figure 2B). Upon phosphorylation, this site accounts for the interaction with class IA phosphoinositide 3-kinases (PI3Ks) which become activated and promote the shift of IDO1 from the cytosol to early endosomes. Herein, the ITIM phosphorylated form of IDO1 acts as a signaling molecule activating genomic effects that lead to long-lasting immunosuppression.^[54]

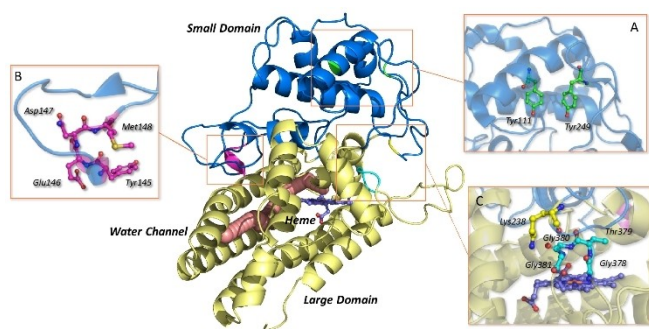


Figure 2. Cartoon structure of IDO1 (PDB code: 6CXU) displaying the large (yellow) and small (blue) domains. Functional ITIM motifs are highlighted in green (box A) and the YENM motif in magenta (box B). Lys238 and the GTGG motif are also evidenced (box C). The tunnel cavity for water/oxygen is shown with orange spheres (Caver 3.0.2, PyMOL).

A flexible loop (DE-loop, residues 260–268) connects the large catalytic domain and the small signaling domain, shaping the catalytic pocket above the sixth coordination site of the heme-iron. The access to this site is governed by a large flexible loop (JK-loop, residues 360–382), whose distinct closed, intermediate and open conformations regulate substrate recognition and binding of inhibitors and heme cofactor to the catalytic site.^[47,55–58] A channel for the shuttling of water and oxygen molecules from/to the catalytic site is shaped by α -helices E and F, extending into the distal and proximal pockets above and below the plane of the heme group, respectively (Figure 2).^[46]

Molecular recognition of L-Trp to IDO1 was investigated using a wide array of studies including biochemical, spectroscopic, biophysical, crystallographic and computational approaches. Specifically, pioneering biochemical studies provided first evidences that high concentrations of L-Trp were able to inhibit the catalytic activity of IDO1.^[38,39] Further spectroscopic and biochemical studies confirmed these early observations, supporting the existence of an inhibitory substrate binding pocket in IDO1 along with the catalytic binding site.^[59–61]

The determination of the crystal structure of IDO1 in complex with L-Trp shed light on the binding modes of the substrate into the active site as well as into the inhibitory binding site.^[46,62]

At micromolar concentration ($< 40 \mu\text{M}$) and following oxygen binding to ferrous IDO1,^[61,63–65] L-Trp occupies the distal pocket above the sixth coordination site of the heme-iron to generate the active ternary complex (Figure 3A). Herein, the nitrogen atom of the indole ring makes a water-mediated hydrogen bond with Ser167, whereas the aromatic moiety engages Phe163 and Tyr126 in face-to-edge π -stacking and hydrophobic interactions, respectively. The aminoacidic moiety of the substrate forms two donating hydrogen bond interactions from its protonated amino group to Thr379 and the negatively charged 7-propionate moiety of the heme, and at least three accepting hydrogen bonds from its carboxylic group to the side chains of Arg231 and Thr379.

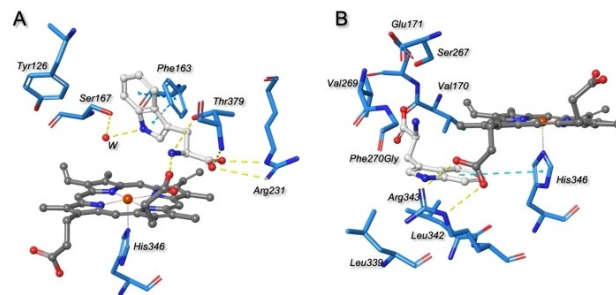


Figure 3. Binding mode of L-Trp into the catalytic cleft (A) and the inhibitory site (B) of hIDO1 (PDB code: 5WMM). Hydrogen bond interactions are shown with yellow dashed lines; π -stacking interactions are shown with blue dashed lines.

Type and number of these interactions are in agreement with those frequently observed for primary amine and carboxylic moieties in the crystal structures of ligand-bound protein complexes.^[66,67] Although Tyr126, Arg231 and Thr379 are conserved in the catalytic site of human TDO (Tyr42, Arg144, Thr342), Ser167 is replaced by a residue of histidine (His76) (Figure S1, Supporting Information).^[45,50]

Since both IDO1 and TDO catalyze the same reaction, the above observation prompted mutagenesis and biochemical studies to investigate the role of Ser167 in the catalytic turnover of IDO1. Early results found that mutants Ser167Ala and Ser167His dampen the enzymatic activity (Table S1, Supporting Information).^[51,68] More recent studies have provided a tentative explanation to this detrimental effect, showing that mutant Ser167His induces conformational changes of Phe270 and His287, and secondary motifs including the DE-loop and EF-loop (residues 277–287).^[65] Collectively, these movements distort the water and oxygen channel which becomes partially occluded, hampering oxygen delivery to the catalytic site.

Thr379 belongs to a conserved GTGG motif of the JK-loop which controls substrate/product shuttling (Figure 2C),^[57] whereas Arg231 was proposed to be part of an electrostatic gate that undertakes inward movement upon binding of the substrate.^[55] Consistent with the importance of these residues in the molecular recognition of L-Trp, mutant Thr379Ala shows a five-fold reduction of the enzymatic activity, whereas mutants Arg231Ala and Arg231Leu abrogate IDO1 activity, albeit not heavily affecting the dissociation constant of the substrate (Table S1, Supporting Information).^[51,57]

Likewise, mutagenesis studies on ancestral IDO1/IDO2 chimeric enzymes disclosed a crucial role of Tyr126 in determining the high affinity of L-Trp to ancestral IDO1 over IDO2.^[69] Conversely, the effect of mutant Phe163Ala was found negligible on the catalytic activity yet significant on the substrate dissociation constant (Table S1, Supporting Information), highlighting the importance of the π -stacking interaction in the molecular recognition of the substrate by IDO1.^[51]

Several proposals have been advanced in literature for the reaction mechanism adopted by IDO1 for the production of NFK (2) in the distal pocket.^[51,70–72] This topic has been thoroughly reviewed elsewhere and is still matter of debate.^[39,73]

Recent works suggest a two-steps reaction mechanism (Figure S2, Supporting Information), with two alternative scenarios for the first step.^[74–79] In particular, the first step is proposed to occur alternatively by (i) electrophilic addition of the lone pair of indole nitrogen to the bound oxygen molecule, or (ii) radical addition. Then, the second step is proposed to occur through a stepwise insertion of oxygen into the indole moiety of L-Trp, followed by the formation of a ferryl heme species and an epoxide intermediate which undergoes to ring opening for the formation of NFK (2).

Beyond the distal pocket, a high concentration of substrate enables L-Trp to occupy both the catalytic site and an inhibitory binding cleft which is located in the proximal pocket below the heme plane. As a consequence, the enzymic activity of IDO1 is dampened giving rise to the long-observed phenomenon of inhibition by substrate.^[38,39] The putative binding mode of L-Trp into the proximal inhibitory pocket was disclosed by crystallographic experiments, using the IDO1 variant Phe270Gly (PDB code: 5WMW; Figure 3B).^[46] It was found that no strong polar interaction is formed between L-Trp and polar residues of the pocket, which include Glu171, Ser267 and Arg343. Conversely, the substrate makes hydrophobic contacts with the heme cofactor and the side chains of Val170, Val269, Leu339 and Leu342. A face-to-edge π -stacking interaction is also observed between the side chain of His346 and the indole ring of L-Trp (Figure 3B). This binding mode is in agreement with the high dissociation constant reported for L-Trp to the inhibitory pocket of ferric IDO1-CN-Trp complex, being in the millimolar range of potency ($K_d = 26$ mM).^[61] While positive allosteric modulators of IDO1 such as indoleamine-ethanol (IDE) and NAS,^[44,46] or some uncompetitive inhibitors such as mitomycin C,^[60] have been observed or proposed to occupy this proximal pocket, recent computational and biophysical studies unveil clues on the existence of additional metastable and putative hidden pockets of L-Trp in the structure of IDO1.^[47]

Specifically, supervised molecular dynamics (suMD) drew a plausible approaching pathway of L-Trp from the solvent to the catalytic site of IDO1, pinpointing a metastable binding site on Lys238 that promotes a first interaction to the substrate (Figure 2C). The conformational plasticity of the JK-loop imparted by Gly378 was also found crucial for the molecular recognition process of L-Trp. These results were supported by mutagenesis experiments in murine P1.HTR cells that found mutants Lys242Met and Gly382Pro (mouse residue numbering) reducing and abrogating the catalytic activity of IDO1, respectively. In the same study, microscale thermophoresis was used to study binding interactions between L-Trp and IDO1 in the catalytically competent heme-bound and apo- states. Notably, multiple binding events of the substrate to the enzyme were found in both states. In particular, low (IDO1, $K_d = 0.31 \pm 0.09$ μ M; apo-IDO1, $K_d = 4.84 \pm 1.48$ μ M) and high (IDO1, $K_d = 574 \pm 73$ μ M; apo-IDO1, $K_d > 6000$ μ M) dissociation constants were detected, suggesting the presence of two distinct binding pockets for L-Trp in the enzyme, whose substrate affinity is affected by the presence/absence of the heme cofactor. Although the high dissociation constant agrees with previous studies on the binding interaction of L-Trp to the catalytic active

site of IDO1 ($K_d = 320$ μ M,^[51] or $K_d = 570$ μ M;^[80] or $K_d = 900$ μ M,^[60,61] the low dissociation constant is not in agreement with the high dissociation constant associated to the binding of the substrate into the inhibitory pocket of the enzyme ($K_d = 26,000$ μ M),^[61] suggesting the existence of a putative *exo* site in the structure of IDO1 yet to be identified.

2.2. IDO2

It is thought that IDO2 and IDO1 are evolutionary orthologs, originating by duplication of an ancestor gene in vertebrates.^[69] Human IDO2 and IDO1 share 42.75% sequence identity (Figure S3, Supporting Information). Although no structural data are available on IDO2, sequence alignment shows that some key residues of substrate binding of IDO1 are conserved in IDO2 sequence. Specifically, residues Phe163, Arg231, Gly378 and Thr379 of the catalytic site, and Lys238 of the metastable binding site, are conserved in both sequences, suggesting a common basis of molecular recognition for the substrate. Notably, Ser167 and Tyr126 are replaced by Thr184 and His143, which account for the poor L-Trp affinity and scarce catalytic activity of IDO2.^[69] Polar and hydrophobic residues of the substrate inhibitory pocket (Glu171, Ser267, Arg343, Val170, Val269, Leu339 and Leu342) are also conserved in IDO2 with the exception of Phe270 that is replaced by a leucine residue. This latter observation combines with a not conserved His287 and a shorter loop connecting α -helices E and F (residues 295–300, Figure S3, Supporting Information), which leads to conjecture a differently shaped water/oxygen channel that may also account for the poor catalytic activity of IDO2 due to a scant oxygen delivery.

2.3. TDO

Human TDO adopts a catalytically active homo-tetrameric form that is assembled as dimer of dimers, with each monomer being composed of twelve α -helices (A–L).^[45,81] Three regions can be identified in the structure: a small N-terminal region (residues 1–65) that contributes to shape the catalytic site of the adjacent monomer in the tetramer (Figure 4); a large region (residues 66–213 and 281–360) holding the heme cofactor, and a C-terminal region (residues 360–382) that is also composed of residues protruding from the large region (residues 214–280) of the enzyme.

In the tetrameric complex, α -helices B, C and J from each monomer form the central part of the interacting interface. Of note, heme binding to human TDO stabilizes the tetrameric form, whereas apo-TDO adopts a dimeric form.^[81] In contrast to the broad substrate specificity of IDO1 toward indole bearing compounds, TDO is endowed with a narrower specificity to L-Trp. The catalytic site is located on the terminal part of the large region of each monomer and is also composed of part of the N-terminal region originating from another adjacent monomer of the tetramer. Although TDO has a distinct evolutionary origin from IDO1,^[82] both enzymes catalyze the same reaction. This

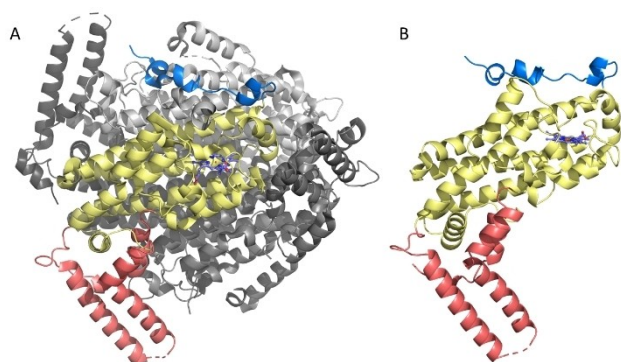


Figure 4. Tetrameric quaternary structure (A) and folding domains (B) of hTDO (PDB code: 5TIA). The small N-terminal region is depicted in blue cartoon; the large region is shown in yellow cartoon; the C-terminal region is pictured in red cartoon.

has led to conjecture a similar reaction mechanism adopted by both enzymes to produce NFK (2).^[84] At odds, recent spectroscopic studies have shown that the steady state behavior of TDO is different from IDO1. In particular, it was found that a ternary complex $[\text{Fe(II)-O}_2, \text{L-Trp}]$ accumulates during TDO steady state,^[83] instead of a ferryl heme species as it occurs in the case of IDO1 (Figure S2, Supporting Information).^[77,79]

The crystal structure of TDO in complex with L-Trp and oxygen unveils the binding mode of the substrate into the catalytic site, as well as into an accessory *exo* pocket (PDB code: 5TIA; Figure 5).^[45] Within the catalytic cleft, the carboxylic group of the aminoacidic moiety of L-Trp makes hydrogen bond interactions with the side chain of Arg144 and the backbone of Thr342, whereas the amino group forms hydrogen bonds with the side chain of Thr342 and the 7-propionate group of the heme. The indole ring engages Phe72, Tyr42 and Tyr45 in face-to-edge π -stacking and hydrophobic interactions, with tyrosine residues that are located on the N-terminal region of the adjacent monomer. The indole nitrogen is also hydrogen bonded with His76. The resulting orientation of L-Trp within the catalytic site places the substrate next to the oxygen molecule

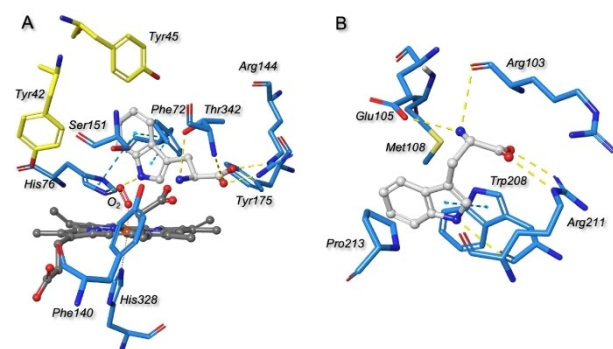


Figure 5. Binding modes of L-Trp into the catalytic cleft (A) and into the allosteric site (B) of hTDO (PDB code: 5TIA). Hydrogen bond interactions are shown with yellow dashed lines; π -stacking interactions are shown with blue dashed lines.

for the catalysis. Specifically, the plane of the indole ring closely approaches the terminal oxygen atom of the co-substrate which is involved in a coordinative bond by the proximal oxygen atom to the heme-iron.

The role of these interactions in substrate binding and catalytic activity has been thoroughly investigated by mutagenesis experiments. Specifically, mutants Tyr42Phe and His76Ala were found to abrogate substrate cooperative binding and reduce the catalytic activity of TDO, respectively.^[85]

In an independent study, site directed mutagenesis of Tyr42, Tyr45 and Arg144 with alanine residues resulted in significant reductions of the catalytic activity, with the mutant forms retaining only 0.50%, 1.13% and 0.88% of the wild type activity.^[50] Furthermore, a complete loss of TDO activity was also observed in variants His76Ala and Phe72Ala. While these results highlight the detrimental effects of deletion of some specific substrate interactions into the catalytic cleft, the additional reported abrogation of catalytic activity by His328Ala as well as its reduction by Phe140Ala and Ser151Ala (Table S1, Supporting Information) find an explanation with the role of the three residues in anchoring the heme cofactor to the protein.

Combining mutagenesis experiments and molecular dynamic simulations, another study found that the hydrogen bond interaction of the substrate with Thr342 is important for the stereospecificity of molecular recognition toward the L- ($K_M = 1.19 \text{ mM}$, $k_{\text{cat}} = 0.101 \text{ s}^{-1}$) over the D-enantiomer ($K_M = 1.59 \text{ mM}$, $k_{\text{cat}} = 0.082 \text{ s}^{-1}$; Table S1, Supporting Information).^[49]

More recently, mutagenesis studies of residue Tyr175 belonging to the EG-loop have found that this region regulates the catalytic turnover of the enzyme, promoting product release ($\text{hTDO}^{\text{WT}} k_{\text{NFK}} = 5.8 \text{ s}^{-1}$; $\text{hTDO}^{\text{Thr175Gly}} k_{\text{NFK}} = 0.9 \text{ s}^{-1}$).^[45]

The binding of L-Trp to the *exo* pocket of TDO features a dissociation constant ($K_d = 0.5 \mu\text{M}$) lower than the catalytic site ($K_d = 54 \mu\text{M}$).^[45] Herein, the carboxylic group of the substrate forms a salt bridge interaction with Arg211, while the amino moiety interacts through hydrogen bonds with Glu105 and the backbone of Arg103. A further hydrogen bond interaction is established between the backbone of Trp208 and the nitrogen atom of the indole ring, with the aromatic part of this moiety also engaging the side chains of Trp208 and Pro213 in aromatic and hydrophobic contacts, respectively. In agreement with these interactions, binding experiments of L-Trp to the double mutant Trp208Val/Arg211Leu resulted in the loss of the low dissociation constant, without perturbing the high dissociation constant that is associated to the interaction with the main catalytic cleft.

Further biochemical and cellular studies showed that the occupancy of the *exo* pocket by L-Trp improves TDO stability against ubiquitin (Ub)-dependent proteasomal degradation.^[45]

Of note, a human disease condition of hypertryptophanemia was found associated to two single nucleotide polymorphisms of TDO, including Met108Ile mutation.^[86] Biochemical and binding studies of L-Trp against Met108Ile mutant showed that this aminoacidic replacement decreases the catalytic activity of the enzyme ($\text{hTDO}^{\text{WT}} K_M = 0.132 \text{ mM}$; $\text{hTDO}^{\text{Met108Ile}} K_M = 0.236 \text{ mM}$) while increasing the proteolytic

degradation of TDO due to a poorer affinity of the substrate to the *exo* pocket (hTDO^{WT} $K_D = 0.11 \mu\text{M}$; hTDO^{Met108Ile} $K_D = 11 \mu\text{M}$).^[86]

At odds with IDO1, it has long been reported that the ferric inactive form of TDO can be activated to the catalytically ferrous active form by hydrogen peroxide in presence of L-Trp.^[87,88] Using Mössbauer and electron paramagnetic resonance spectroscopy, the mechanism of TDO reactivation by hydrogen peroxide and L-Trp has been more recently proposed, showing that the substrate acts as reductant for the enzyme.^[89] Specifically, the enzyme reactivation pathway proceeds with the hydrogen peroxide triggering the formation of a reaction intermediate which is composed of a ferryl species and a protein-based free radical. This intermediate is then reduced by L-Trp leading to the catalytically ferrous active form of TDO. The reactivation mechanism may allow the activation of TDO in oxidizing environments such as those found in the hepatocytes, wherein the enzyme is mostly expressed.

3. Structure and Substrate Binding Pockets of Tryptophan Hydroxylases

3.1. TPH1

TPH1 is a homo-tetramer belonging to the family of aromatic amino acid hydroxylases.^[90] It is composed of three functional domains: a N-terminal regulatory domain being able to dimerize,^[91] a central conserved catalytic domain, and a C-terminal oligomerization domain.

The reaction mechanism of tryptophan hydroxylation proceeds with two coupled steps.^[92] In the first step, the reaction among tetrahydrobiopterin (BH₄) cofactor, oxygen and catalytic site iron leads to the formation of an iron peroxypterin intermediate. Then, the insertion of oxygen into position C5 of L-Trp occurs in the second step of the reaction (Figure S2, Supporting Information), so that a molecule of product (12) is formed for each molecule of BH₄ being oxidized.

Although no structural information is still available for the N-terminal and C-terminal domains of human TPH1, the first structure of its catalytic domain was released in 2002 in complex with the cofactor 7,8-dihydro-L-biopterin (BH₂) and iron (Fe³⁺) (PDB code: 1MLW; Figure 6A).^[93]

Since then, other crystallographic studies followed solving different inhibitor-bound complexes of human TPH1 (hTPH1) catalytic domain.^[94–96] Yet, only the atomic coordinates of the chicken isoform (cTPH1; PDB code: 3E2T) are available for the substrate-bound structure that show also an iron-bound imidazole in the active site.^[97] The two species specific isoforms share high sequence identity (85.8%) and conserved binding site residues (Figure S4, Supporting Information). As a consequence, the binding mode of L-Trp to cTPH1 can be discussed assuming that it may also be conserved into the catalytic cleft of hTPH1 (Figure 6B). In particular, the carboxylic group of L-Trp makes a salt bridge with Arg258 and hydrogen bonds with the side chain of Ser337 and the amide backbone of Thr266. A π -

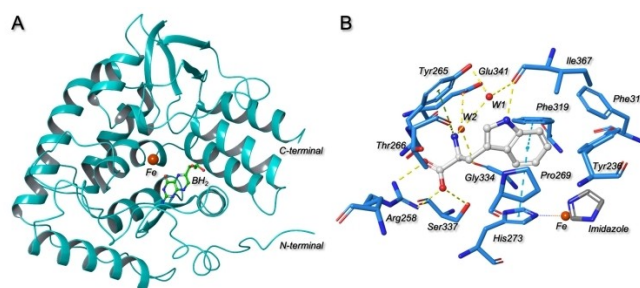


Figure 6. Catalytic domain of hTPH1 (A; PDB code: 1MLW) and the binding mode of L-Trp into the binding site of cTPH1 (B; PDB code: 3E2T). Hydrogen bond interactions are shown with yellow dashed lines; π -stacking interactions are shown with blue dashed lines.

cation interaction is observed between the side chain of Tyr265 and the protonated amino group of the substrate, which also forms hydrogen bonds with two water molecules and the carbonyl backbone of Thr266. The indole ring engages the side chains of His273, Tyr236, Phe314 and Phe319 in face-to-edge π -stacking interactions, whereas making hydrophobic contacts with Ile367 and Pro269. An important role in substrate binding is also played by two water molecules which allow bridge interactions of the substrate with Tyr265, Gly334, and Glu341 through a hydrogen bond network.

Mutagenesis experiments confirmed the important roles of Tyr236 and Phe314 in substrate binding and specificity.^[98–100]

Specifically, Tyr236Ala and Tyr236Leu mutants show a decrease of substrate binding, whereas Phe314Trp variant broadens substrate specificity. A further conserved residue, namely Pro403 in the C-terminal domain, was found to reduce the catalytic activity of murine TPH1 and TPH2 (Pro447) when mutated into an arginine residue,^[101] as a result of a single-nucleotide polymorphism.^[102]

Two phosphorylation sites have been identified in the sequence of hTPH1 on Ser58 for cyclic AMP-dependent protein kinase (PKA), and Ser260 for calcium calmodulin-dependent protein kinase II (CaMKII).^[98,103,104] Although the functional outcome of Ser260 phosphorylation is still elusive,^[98] phosphorylation by PKA of Ser58 within the regulatory domain of the enzyme has been associated to the activation of hTPH1.^[103]

3.2. TPH2

Although hTPH2 and hTPH1 are encoded by two different genes, the primary sequence of hTPH2 shares an overall identity of 63.8% with hTPH1 (Figure S4, Supporting Information) and a conserved structural architecture which is composed of three functional domains.^[8,70] Only one crystal structure is available for the catalytic domain of human TPH2 (PDB code: 4V06), albeit no supporting paper has been published yet. No ligand is co-crystallized into this structure, except for the imidazole molecule and an iron atom (Fe³⁺).

Since binding site residues of hTPH2 are conserved in cTPH1 and hTPH1 (Figure S4, Supporting Information), it may

again be suggested that a conserved binding mode of L-Trp exist among the catalytic clefts of these enzymatic isoforms (Figure 6B).

Notably, hTPH2 contains a functional phosphorylation site on Ser19 of the N-terminal regulatory domain that promotes enzyme activation by CaMKII.^[105,106] This site is not conserved in the human and chicken isoforms of TPH1, but it is present in the sequence of cTPH2 (Figure S4, Supporting Information). Upon phosphorylation, hTPH2 is able to interact with 14–3–3 proteins increasing its protein stability and catalytic activity.^[106]

4. Conformational Properties of L-Trp

Molecular recognition of a substrate to its cognate enzyme is a complex and dynamic event that involves the conformational rearrangement of both binding partners according to their energetic landscapes.^[107] The binding of a substrate to its protein target determines a restriction of the conformational freedom to a bioactive conformation that may be different from the global energy minimum of the solvated ligand.^[108,109]

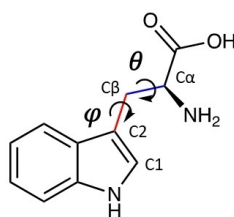


Figure 7. Torsional angles of L-Trp considered for the generation of the conformational profile. The dihedral angle θ (N-C α -C β -C2) and dihedral angle ϕ (C α -C β -C2-C1) are colored in blue and red, respectively.

Conf.	θ [°]	ϕ [°]	Solution Phase Energy (Hartree)	ΔE global min. [kcal mol ⁻¹]
#1	55.4	86.2	-686.4095	0.439
#2	48.9	264.4	-686.4102	0.000
#3	295.2	273.5	-686.4084	1.130
#4	296.8	106.4	-686.4098	0.251

A recent study has shown that conformational preferences and energetics in molecular recognition between ligand and protein cognate partners are primarily determined by intrinsic barrier to rotation around single bonds of ligand, and that ligand/target intermolecular interactions have a minor role in determining the bioactive conformation.^[110]

In this paragraph we discuss the conformational properties of L-Trp and its conformational preferences in the recognition of the cognate enzymes IDO1, TDO, and TPH1. The conformational profile of L-Trp is determined by two torsional angles (θ and ϕ , Figure 7).

Employing a molecular mechanic approach, a systematic rotation of each of these angles from 0° to 360°, with an increment of 1°, allows the generation of a total of 130,321 theoretical conformers (see methods in Supporting Information). These conformations were energetically minimized using quantum chemistry calculations, yielding the identification of four distinct energetic minima (Table 2).

Energetic levels of the bioactive conformations of L-Trp extracted from available crystallographic data were determined placing energetic constraints on the torsional angles θ and ϕ , and refining bond stretching energies with quantum chemistry calculations. The inspection of results shows that IDO1 and TDO recognize the same bioactive conformation of the substrate into the catalytic site (Table 3 and Table 4, conf. #4).

Although this observation is in agreement with the common biochemical reaction that both enzymes adopt for the oxidative cleavage of the indole ring of L-Trp, it does not explain the lower K_M value of the substrate to hIDO1 than hTDO (Table 1).

Hence, additional enthalpic and entropic factors may account for a different K_M value of L-Trp into the catalytic clefts of hIDO1 and hTDO, which are determined by specific non-conserved structural features of these two enzymes. Notably, this bioactive conformation is distinct from those conformations adopted by L-Trp to occupy the proximal inhibitory pocket of IDO1 (Table 3, conf. #2) or the *exo* site of TDO (Table 4, conf. #3). Hence, medicinal chemistry strategies may be envisaged aimed at constraining θ and ϕ angles to yield conformational restricted analogues of L-Trp that selectively bind to the proximal inhibitory pocket of IDO1 or the *exo* site of TDO. In the case of TPH1, L-Trp adopts a bioactive conformation that is very close to its global minimum (Table 4, conf. #2), which may in

PDB	Site	ΔE global min. [kcal mol ⁻¹]	#1[Å]	#2[Å]	#3[Å]	#4[Å]
5WMX ^[a]	Cat.	1.890	1.775	1.739	2.271	0.694
5WMW ^[a]	Cat.	4.554	1.700	1.881	2.369	0.530
5WMU	Cat.	1.674	1.664	1.917	2.413	0.451
5WMV	Cat.	1.692	1.632	1.907	2.416	0.522
6E46 ^[b]	Cat.	1.998	1.949	1.732	2.103	1.020
6E35	Cat.	1.843	1.679	1.887	2.406	0.440
6CXU ^[c]	Cat.	2.004	1.780	1.776	2.290	0.638
6CXV ^[c]	Cat.	2.195	1.794	1.792	2.293	0.618
5WMW ^[a]	Inhib	1.194	2.428	0.289	1.527	1.877

[a] hIDO1 mutant F270G. [b] hIDO1 mutant K118 A, K199 A. [c] hIDO1 mutant S157H.

Table 4. Torsional properties (θ and ϕ angles), energetic and RMSD values of L-Trp bioactive conformations binding to hTDO (5TIA) and cTPH1 (3E2T).

PDB	Site	ΔE global min. [kcal mol ⁻¹]	#1 [Å]	#2 [Å]	#3 [Å]	#4 [Å]
5TIA(A)	Cat.	2.413	1.942	1.666	2.107	0.946
5TIA(B)	Cat.	1.760	1.829	1.791	2.220	0.850
5TIA(C)	Cat.	2.134	1.859	1.707	2.193	0.817
5TIA(D)	Cat.	2.192	1.861	1.712	2.195	0.805
5TIA(A)	exo	0.753	3.016	1.693	0.274	2.535
5TIA(B)	exo	0.811	3.008	1.696	0.349	2.515
5TIA(C)	exo	1.561	3.008	1.726	0.367	2.526
5TIA(D)	exo	1.063	3.015	1.706	0.285	2.538
3E2T	Cat.	0.878	2.560	0.278	1.492	1.985

part explain the low K_M value of the substrate toward this enzyme (Table 1).

5. Conclusions

L-Trp is an essential aminoacidic nutrient for human body that is exploited for protein synthesis and production of important bioactive metabolites. This latter occurs at the crossroads of the kynurenine and serotonin pathways, wherein IDO1, TDO, TPH1 and TPH2 constitute pivotal enzymes regulating a wide array of physiological functions in CNS and peripheral tissues through consumption of L-Trp and production of downstream signalling molecules. In this review article, we have surveyed structural aspects and recognition patterns of these enzymes toward L-Trp, as hitherto unveiled by crystallographic studies, biophysical and computational works available in scientific literature. Collectively, these studies depict a scenario representing such enzymes as sophisticated protein machineries containing different hot spots for enzymic and non-enzymic regulatory functions. These hot spots come as accessory binding pockets complementing the main catalytic site for the substrate, or as specific phosphorylation sites that are localized on distinct domains of the protein. The advancements that such studies bring in the scientific community is proving of utmost importance to fully exploit the potential of IDO1, TDO, TPH1 and TPH2 as targets for the development of new drugs in distinct therapeutic areas.

Supporting Information

Table S1: Michaelis-Menten constants, catalytic rate and dissociation constants of L-Trp to mutant forms of hIDO1 and hTDO. Figure S1: Pairwise alignment between the primary sequences of hIDO1 and hTDO. Figure S2: Reaction mechanisms of tryptophan oxidation (A; Scheme adapted from Ref. [83]) and tryptophan hydroxylation (B; Scheme adapted from Ref. [92]). Figure S3: Pairwise alignment between the primary sequences of hIDO1 and hIDO2. Figure S4: Multiple alignment between the primary sequences of hTPH2, cTPH2, cTPH1 and hTPH1. Computational methods for the conformational analysis.

Acknowledgements

We gratefully acknowledge the support of the University of Perugia (Ricerca di base 2020) to Emidio Camaioni and Antonio Macchiarulo. Open Access Funding provided by Università degli Studi di Perugia within the CRUI-CARE Agreement.

Conflict of Interest

The authors declare no conflict of interest.

Keywords: Tryptophan · IDO · TDO · TPH · Molecular Recognition

- [1] F. G. Hopkins, S. W. Cole, *J. Physiol.* **1901**, *27*, 418–428.
- [2] S. Comai, A. Bertazzo, M. Brughera, S. Crotti, *Adv. Clin. Chem.* **2020**, *95*, 165–218.
- [3] S. Palmer, *Eur. J. Clin. Nutr.* **1990**, *44*, 13–21.
- [4] D. J. Millward, *Proc. Nutr. Soc.* **1999**, *58*, 249–260.
- [5] D. A. Bender, *Br. J. Nutr.* **1983**, *50*, 25–32.
- [6] A. Frazer, J. Hensler, *Basic Neurochem.* **1999**, 1–5.
- [7] M. Berger, J. A. Gray, B. L. Roth, *Annu. Rev. Med.* **2009**, *60*, 355–366.
- [8] J. McKinney, P. M. Knappskog, J. Haavik, *J. Neurochem.* **2005**, *92*, 311–320.
- [9] F. Côté, E. Thévenot, C. Fligny, Y. Fromes, M. Darmon, M. A. Ripoché, E. Bayard, N. Hanoun, F. Saurini, P. Lechat, L. Dandolo, M. Hamon, J. Mallet, G. Vodjdani, *Proc. Natl. Acad. Sci. USA* **2003**, *100*, 13525–13530.
- [10] P. Amireault, D. Sibon, F. Côté, *ACS Chem. Neurosci.* **2013**, *4*, 64–71.
- [11] Z. Li, A. Chalazonitis, Y. Y. Huang, J. J. Mann, K. G. Margolis, Q. M. Yang, D. O. Kim, F. Côté, J. Mallet, M. D. Gershon, *J. Neurosci.* **2011**, *31*, 8998–9009.
- [12] K. B. Neal, L. J. Parry, J. C. Bornstein, *J. Physiol.* **2009**, *587*, 567–586.
- [13] K. Waløen, R. Kleppe, A. Martinez, J. Haavik, *Expert Opin. Ther. Targets* **2017**, *21*, 167–180.
- [14] G. Cianchetta, T. Stouch, W. Yu, Z. C. Shi, L. W. Tari, R. V. Swanson, M. J. Hunter, I. D. Hoffman, Q. Liu, *Curr. Chem. Genomics* **2010**, *4*, 19–26.
- [15] A. Markham, *Drugs* **2017**, *77*, 793–798.
- [16] A. A. B. Badawy, *Int. J. Tryptophan Res.* **2017**, *10*, 1–10.
- [17] Y. Chen, G. J. Guillemin, *Int. J. Tryptophan Res.* **2009**, *2*, S2097.
- [18] A. Bessede, M. Gargaro, M. T. Pallotta, D. Matino, G. Servillo, C. Brunacci, S. Biciato, E. M. C. Mazza, A. Macchiarulo, C. Vacca, R. Iannitti, L. Tissi, C. Volpi, M. L. Belladonna, C. Orabona, R. Bianchi, T. V. Lanz, M. Platten, M. A. Della Fazio, D. Piobbico, T. Zelante, H. Funakoshi, T. Nakamura, D. Gilot, M. S. Denison, G. J. Guillemin, J. B. DuHadaway, G. C. Prendergast, R. Metz, M. Geffard, L. Boon, M. Pirro, A. Iorio, B. Veyret, L. Romani, U. Grohmann, F. Fallarino, P. Puccetti, *Nature* **2014**, *511*, 184–190.
- [19] C. A. Opitz, U. M. Litzenburger, F. Sahm, M. Ott, I. Tritschler, S. Trump, T. Schumacher, L. Jestaedt, D. Schrenk, M. Weller, M. Jugold, G. J.

- Guillemin, C. L. Miller, C. Lutz, B. Radlwimmer, I. Lehmann, A. Von Deimling, W. Wick, M. Platten, *Nature* **2011**, *478*, 197–203.
- [20] N. T. Nguyen, A. Kimura, T. Nakahama, I. Chinen, K. Masuda, K. Nohara, Y. Fujii-Kuriyama, T. Kishimoto, *Proc. Nat. Acad. Sci.* **2010**, *107*, 19961–19966.
- [21] J. D. Mezrich, J. H. Fechner, X. Zhang, B. P. Johnson, W. J. Burlingham, C. A. Bradfield, *J. Immunol.* **2010**, *185*, 3190–3198.
- [22] T. W. Stone, L. G. Darlington, *Nat. Rev. Drug Discovery* **2002**, *1*, 609–620.
- [23] A. L. Colín-González, P. D. Maldonado, A. Santamaría, *Neurotoxicology* **2013**, *34*, 189–204.
- [24] L. E. Goldstein, M. C. Leopold, X. Huang, C. S. Atwood, A. J. Saunders, M. Hartshorn, J. T. Lim, K. Y. Faget, J. A. Muffat, R. C. Scarpa, L. T. Chylack, E. F. Bowden, R. E. Tanzi, A. I. Bush, *Biochemistry* **2000**, *39*, 7266–7275.
- [25] R. S. Grant, S. E. Coggan, G. A. Smythe, *Int. J. Tryptophan Res.* **2009**, *2*, 71–79.
- [26] M. C. Bosco, A. Rapisarda, G. Reffo, S. Massazza, S. Pastorino, L. Varesio, *Adv. Exp. Med. Biol.* **2003**, *527*, 55–65.
- [27] A. B. Dounay, J. B. Tuttle, P. R. Verhoest, *J. Med. Chem.* **2015**, *58*, 8762–8782.
- [28] L. Vécsei, L. Szalardy, F. Fülöp, J. Toldi, *Nat. Rev. Drug Discovery* **2013**, *12*, 64–82.
- [29] T. Biernacki, D. Sandi, K. Bencsik, L. Vécsei, *Cells* **2020**, *9*, 1564.
- [30] Y. S. Huang, J. Ogbechi, F. I. Clanchy, R. O. Williams, T. W. Stone, *Front. Immunol.* **2020**, *11*, 388.
- [31] B. Cao, Y. Chen, Z. Ren, Z. Pan, R. S. McIntyre, D. Wang, *Neurosci. Biobehav. Rev.* **2021**, *123*, 203–214.
- [32] S. A. Rafice, N. Chauhan, I. Efimov, J. Basran, E. L. Raven, *Biochem. Soc. Trans.* **2009**, *37*, 408–412.
- [33] A. Macchiarulo, E. Camaioni, R. Nuti, R. Pellicciari, *Amino Acids* **2009**, *37*, 219–229.
- [34] A. Coletti, F. A. Greco, D. Dolciame, E. Camaioni, R. Sardella, M. T. Pallotta, C. Volpi, C. Orabona, U. Grohmann, A. Macchiarulo, *MedChemComm* **2017**, *8*, 1378–1392.
- [35] Z. Ye, L. Yue, J. Shi, M. Shao, T. Wu, *J. Cancer* **2019**, *10*, 2771–2782.
- [36] A. Kozlova, R. Frédérick, *Expert Opin. Ther. Pat.* **2019**, *29*, 11–23.
- [37] M. W. Taylor, G. Feng, *FASEB J.* **1991**, *5*, 2516–2522.
- [38] M. Sono, T. Taniguchi, Y. Watanabe, O. Hayaishi, *J. Biol. Chem.* **1980**, *255*, 1339–1345.
- [39] M. Sono, M. P. Roach, E. D. Coulter, J. H. Dawson, *Chem. Rev.* **1996**, *96*, 2841–2887.
- [40] H. J. Ball, H. J. Yuasa, C. J. D. Austin, S. Weiser, N. H. Hunt, *Int. J. Biochem. Cell Biol.* **2009**, *41*, 467–471.
- [41] U. Grohmann, *Trends Immunol.* **2003**, *24*, 242–248.
- [42] A. L. Mellor, D. H. Munn, *Nat. Rev. Immunol.* **2004**, *4*, 762–774.
- [43] H. J. Ball, A. Sanchez-Perez, S. Weiser, C. J. D. Austin, F. Astelbauer, J. Miu, J. A. McQuillan, R. Stocker, L. S. Jermini, N. H. Hunt, *Gene* **2007**, *396*, 203–213.
- [44] G. Mondanelli, A. Coletti, F. A. Greco, M. T. Pallotta, C. Orabona, A. Iacono, M. L. Belladonna, E. Albin, E. Panfil, F. Fallarino, M. Gargaro, G. Manni, D. Martino, A. Carvalho, C. Cunha, P. Maciel, M. Di Filippo, L. Gaetani, R. Bianchi, C. Vacca, I. M. Iamandii, E. Proietti, F. Boscia, L. Annunziato, M. Peppelenbosch, P. Puccetti, P. Calabresi, A. Macchiarulo, L. Santambrogio, C. Volpi, U. Grohmann, *Proc. Natl. Acad. Sci. USA* **2020**, *117*, 3848–3857.
- [45] A. Lewis-Ballester, F. Frouhar, S. M. Kim, S. Lew, Y. Wang, S. Karkashon, J. Seetharaman, D. Batabyal, B. Y. Chiang, M. Hussain, M. A. Correia, S. R. Yeh, L. Tong, *Sci. Rep.* **2016**, *6*, 1–13.
- [46] A. Lewis-Ballester, K. N. Pham, D. Batabyal, S. Karkashon, J. B. Bonanno, T. L. Poulos, S. R. Yeh, *Nat. Commun.* **2017**, *8*, 1693.
- [47] F. A. Greco, E. Albin, A. Coletti, D. Dolciame, A. Carotti, C. Orabona, U. Grohmann, A. Macchiarulo, *ChemMedChem* **2019**, *14*, 2084–2092.
- [48] J. Basran, S. A. Rafice, N. Chauhan, I. Efimov, M. R. Cheesman, L. Ghamsari, E. L. Raven, *Biochemistry* **2008**, *47*, 4752–4760.
- [49] L. Capece, A. Lewis-Ballester, M. A. Marti, D. A. Estrin, S. R. Yeh, *Biochemistry* **2011**, *50*, 10910–10918.
- [50] B. Meng, D. Wu, J. Gu, S. Ouyang, W. Ding, Z. J. Liu, *Proteins Struct. Funct. Bioinf.* **2014**, *82*, 3210–3216.
- [51] H. Sugimoto, S. I. Oda, T. Otsuki, T. Hino, T. Yoshida, Y. Shiro, *Proc. Natl. Acad. Sci. USA* **2006**, *103*, 2611–2616.
- [52] A. Mammoli, A. Coletti, M. Ballarotto, A. Riccio, A. Carotti, U. Grohmann, E. Camaioni, A. Macchiarulo, *ChemMedChem* **2020**, *15*, 891–899.
- [53] E. Albin, V. Rosini, M. Gargaro, G. Mondanelli, M. L. Belladonna, M. T. Pallotta, C. Volpi, F. Fallarino, A. Macchiarulo, C. Antognelli, R. Bianchi, C. Vacca, P. Puccetti, U. Grohmann, C. Orabona, *J. Cell. Mol. Med.* **2017**, *21*, 165–176.
- [54] A. Iacono, A. Pompa, F. De Marchis, E. Panfil, F. A. Greco, A. Coletti, C. Orabona, C. Volpi, M. L. Belladonna, G. Mondanelli, E. Albin, C. Vacca, M. Gargaro, F. Fallarino, R. Bianchi, C. De Marcos Lousa, E. M. Mazza, S. Biciato, E. Proietti, F. Milano, M. P. Martelli, I. M. Iamandii, M. Graupera Garcia-Mila, J. Llena Sopena, P. Hawkins, S. Suire, K. Okkenhaug, A. Stark, F. Grassi, M. Bellucci, P. Puccetti, L. Santambrogio, A. Macchiarulo, U. Grohmann, M. T. Pallotta, *EMBO Rep.* **2020**, *21*, e49756.
- [55] A. Macchiarulo, R. Nuti, D. Bellocchi, E. Camaioni, R. Pellicciari, *Biochim. Biophys. Acta Proteins Proteomics* **2007**, *1774*, 1058–1068.
- [56] F. A. Greco, A. Bourinque, A. Coletti, C. Custodi, D. Dolciame, A. Carotti, A. Macchiarulo, *Mol. Inf.* **2016**, *35*, 449–459.
- [57] L. Álvarez, A. Lewis-Ballester, A. Roitberg, D. A. Estrin, S. R. Yeh, M. A. Marti, L. Capece, *Biochemistry* **2016**, *55*, 2785–2793.
- [58] M. Mirgoux, L. Leherter, J. Wouters, *Acta Crystallogr. Sect. D* **2020**, *76*, 1211–1221.
- [59] E. Nickel, K. Nienhaus, C. Lu, S. R. Yeh, G. U. Nienhaus, *J. Biol. Chem.* **2009**, *284*, 31548–31554.
- [60] C. Lu, Y. Lin, S. R. Yeh, *J. Am. Chem. Soc.* **2009**, *131*, 12866–12867.
- [61] C. Lu, Y. Lin, S. R. Yeh, *Biochemistry* **2010**, *49*, 5028–5034.
- [62] S. Luo, K. Xu, S. Xiang, J. Chen, C. Chen, C. Guo, Y. Tong, L. Tong, *Acta Crystallogr. Sect. F* **2018**, *74*, 717–724.
- [63] I. Efimov, J. Basran, X. Sun, N. Chauhan, S. K. Chapman, C. G. Mowat, E. L. Raven, *J. Am. Chem. Soc.* **2012**, *134*, 3034–3041.
- [64] A. O. Kolawole, B. P. Hixon, L. S. Dameron, I. M. Chrisman, V. V. Smirnov, *Arch. Biochem. Biophys.* **2015**, *570*, 47–57.
- [65] A. Lewis-Ballester, S. Karkashon, D. Batabyal, T. L. Poulos, S. R. Yeh, *J. Am. Chem. Soc.* **2018**, *140*, 8518–8525.
- [66] A. Macchiarulo, R. Nuti, G. Eren, R. Pellicciari, *J. Chem. Inf. Model.* **2009**, *49*, 900–912.
- [67] A. Macchiarulo, R. Pellicciari, *J. Mol. Graphics Modell.* **2007**, *26*, 728–739.
- [68] N. Chauhan, J. Basran, I. Efimov, D. A. Svistunenko, H. E. Seward, P. C. E. Moody, E. L. Raven, *Biochemistry* **2008**, *47*, 4761–4769.
- [69] H. J. Yuasa, *FEBS J.* **2016**, *283*, 3651–3661.
- [70] G. A. Hamilton, *Adv. Enzymol. Relat. Areas Mol. Biol.* **1969**, *32*, 55–96.
- [71] O. Hayaishi, S. Rothberg, A. H. Mehler, Y. Saito, *J. Biol. Chem.* **1957**, *229*, 889–896.
- [72] A. C. Terentis, S. R. Thomas, O. Takikawa, T. K. Littlejohn, R. J. W. Truscott, R. S. Armstrong, S. R. Yeh, R. Stocker, *J. Biol. Chem.* **2002**, *277*, 15788–15794.
- [73] I. Efimov, J. Basran, S. J. Thackray, S. Handa, C. G. Mowat, E. L. Raven, *Biochemistry* **2011**, *50*, 2717–2724.
- [74] L. W. Chung, X. Li, H. Sugimoto, Y. Shiro, K. Morokuma, *J. Am. Chem. Soc.* **2008**, *130*, 12299–12309.
- [75] N. Chauhan, S. J. Thackray, S. A. Rafice, G. Eaton, M. Lee, I. Efimov, J. Basran, P. R. Jenkins, C. G. Mowat, S. K. Chapman, E. L. Raven, *J. Am. Chem. Soc.* **2009**, *131*, 4186–4187.
- [76] L. Capece, A. Lewis-Ballester, D. Batabyal, N. Di Russo, S. R. Yeh, D. A. Estrin, M. A. Marti, *J. Biol. Inorg. Chem.* **2010**, *15*, 811–823.
- [77] A. Lewis-Ballester, D. Batabyal, T. Egawa, C. Lu, Y. Lin, M. A. Marti, L. Capece, D. A. Estrin, S. R. Yeh, *Proc. Natl. Acad. Sci. USA* **2009**, *106*, 17371–17376.
- [78] L. W. Chung, X. Li, H. Sugimoto, Y. Shiro, K. Morokuma, *J. Am. Chem. Soc.* **2010**, *132*, 11993–12005.
- [79] E. S. Booth, J. Basran, M. Lee, S. Handa, E. L. Raven, *J. Biol. Chem.* **2015**, *290*, 30924–30930.
- [80] N. D. Papadopoulou, M. Mewies, K. J. McLean, H. E. Seward, D. A. Svistunenko, A. W. Munro, E. L. Raven, *Biochemistry* **2005**, *44*, 14318–14328.
- [81] B. Meng, D. Wu, J. Gu, S. Ouyang, W. Ding, Z. J. Liu, *Proteins Struct. Funct. Bioinf.* **2014**, *82*, 3210–3216.
- [82] H. J. Yuasa, H. J. Ball, *J. Exp. Zool. Part B* **2015**, *324*, 128–140.
- [83] J. Basran, E. S. Booth, M. Lee, S. Handa, E. L. Raven, *Biochemistry* **2016**, *55*, 6743–6750.
- [84] S. J. Thackray, G. C. Mowat, S. K. Chapman, *Biochem. Soc. Trans.* **2008**, *36*, 1120–1123.
- [85] E. Fukumura, H. Sugimoto, Y. Misumi, T. Ogura, Y. Shiro, *J. Biochem.* **2009**, *145*, 505–515.
- [86] P. Ferreira, I. Shin, I. Sosova, K. Dornevil, S. Jain, D. Dewey, F. Liu, A. Liu, *Mol. Genet. Metab.* **2017**, *120*, 317–324.
- [87] W. E. Knox, A. H. Mehler, *J. Biol. Chem.* **1950**, *187*, 19–30.
- [88] T. Tanaka, W. E. Knox, *J. Biol. Chem.* **1959**, *234*, 1162–1170.
- [89] R. Fu, R. Gupta, J. Geng, K. Dornevil, S. Wang, Y. Zhang, M. P. Hendrich, A. Liu, *J. Biol. Chem.* **2011**, *286*, 26541–26554.

- [90] P. F. Fitzpatrick, *Annu. Rev. Biochem.* **1999**, *68*, 355–381.
- [91] S. Zhang, C. S. Hinck, P. F. Fitzpatrick, *Biochem. Biophys. Res. Commun.* **2016**, *476*, 457–461.
- [92] K. M. Roberts, P. F. Fitzpatrick, *IUBMB Life.* **2013**, *65*, 350–357.
- [93] L. Wang, H. Erlandsen, J. Haavik, P. M. Knappskog, R. C. Stevens, *Biochemistry* **2002**, *41*, 12569–12574.
- [94] H. Jin, G. Cianchetta, A. Devasagayaraj, K. Gu, B. Marinelli, L. Samala, S. Scott, T. Stouch, A. Tunoori, Y. Wang, Y. Zang, C. Zhang, S. David Kimball, A. J. Main, Z. M. Ding, W. Sun, Q. Yang, X. Q. Yu, D. R. Powell, A. Wilson, Q. Liu, Z. C. Shi, *Bioorg. Med. Chem. Lett.* **2009**, *19*, 5229–5232.
- [95] D. R. Goldberg, S. De Lombaert, R. Aiello, P. Bourassa, N. Barucci, Q. Zhang, V. Paralkar, A. J. Stein, J. Valentine, W. Zavadski, *Bioorg. Med. Chem. Lett.* **2016**, *26*, 2855–2860.
- [96] D. R. Goldberg, S. De Lombaert, R. Aiello, P. Bourassa, N. Barucci, Q. Zhang, V. Paralkar, A. J. Stein, M. Holt, J. Valentine, W. Zavadski, *Bioorg. Med. Chem. Lett.* **2017**, *27*, 413–419.
- [97] M. S. Windahl, C. R. Petersen, H. E. M. Christensen, P. Harris, *Biochemistry* **2008**, *47*, 12087–12094.
- [98] G. C. T. Jiang, G. J. Yohrling, I. V. J. D. Schmitt, K. E. Vrana, *J. Mol. Biol.* **2000**, *302*, 1005–1017.
- [99] J. McKinney, K. Teigen, N. Å. Frøystein, C. Salaün, P. M. Knappskog, J. Haavik, A. Martínez, *Biochemistry* **2001**, *40*, 15591–15601.
- [100] S. C. Daubner, G. R. Moran, P. F. Fitzpatrick, *Biochem. Biophys. Res. Commun.* **2002**, *292*, 639–641.
- [101] S. A. Sakowski, T. J. Geddes, D. M. Kuhn, *J. Neurochem.* **2006**, *96*, 758–765.
- [102] X. Zhang, J. M. Beaulieu, T. D. Sotnikova, R. R. Gainetdinov, M. G. Caron, *Science* **2004**, *305*, 217.
- [103] D. M. Kuhn, R. Arthur, J. C. States, *J. Neurochem.* **1997**, *68*, 2220–2223.
- [104] S. C. Kumer, S. M. Mockus, P. J. Rucker, K. E. Vrana, *J. Neurochem.* **1997**, *69*, 1738–1745.
- [105] D. M. Kuhn, S. A. Sakowski, T. J. Geddes, C. Wilkerson, J. W. Haycock, *J. Neurochem.* **2007**, *103*, 1567–73.
- [106] I. Winge, J. A. McKinney, M. Ying, C. S. D'Santos, R. Kleppe, P. M. Knappskog, J. Haavik, *Biochem. J.* **2008**, *410*, 195–204.
- [107] A. Macchiarulo, I. Nobeli, J. M. Thornton, *Nat. Biotechnol.* **2004**, *22*, 1039–1045.
- [108] E. Perola, P. S. Charifson, *J. Med. Chem.* **2004**, *47*, 2499–2510.
- [109] A. Gioiello, F. Venturoni, S. Tamimi, C. Custodi, R. Pellicciari, A. Macchiarulo, *MedChemComm* **2014**, *5*, 750–757.
- [110] B. K. Rai, V. Sresht, Q. Yang, R. Unwalla, M. Tu, A. M. Mathiowetz, G. A. Bakken, *J. Chem. Inf. Model.* **2019**, *59*, 4195–4208.
- [111] D. Batabyal, S. R. Yeh, *J. Am. Chem. Soc.* **2007**, *129*, 15690–15701.
- [112] O. Takikawa, T. Kuroiwa, F. Yamazaki, R. Kido, *J. Biol. Chem.* **1988**, *263*, 2041–2048.
- [113] G. Pantouris, M. Serys, H. J. Yuasa, H. J. Ball, C. G. Mowat, *Amino Acids* **2014**, *46*, 2155–2163.

Manuscript received: June 5, 2021
Revised manuscript received: June 14, 2021
Accepted manuscript online: June 17, 2021
Version of record online: July 16, 2021